

Experimental Investigation of Parabolic Trough Solar Collector using Receiver with Two-Gate Helical Screw-Tape

R. F. Ahmed*, W. M. El-Awady^a, E. B. Zeidan^a, M. M. Awad^a, G. I. Sultan^a

Abstract— A parabolic trough solar collector (PTC), with two-gate helical screw-tape inserted into an evacuated tube (ET) receiver, is designed and manufactured. The novel helps to increase the heat transfer rate by using the two-pass fluid flow and also by generating a swirl flow. The experiments are performed at flow rates of 10, 12, 16, 20, and 25 L/h. Results showed that the maximum daily efficiency is 69% at water flow rate of 20 L/h while the minimum daily efficiency is 59.5% at water flow rate of 16 L/h. The heat removal factor and the overall heat loss coefficient of the system are 0.843 and 9.64 W/m² °C, respectively. It is also found that the helical screw core enhances the solar collector performance during cloudy periods by compensating the effect of the large instantaneous variation of the incident solar radiation where it works as a thermal storage element.

Keywords— Parabolic trough solar collector (PTC), Evacuated tube (ET) Receiver, Two-gate helical screw, Solar energy.

1 Introduction

I. *Raed Fuaad Ahmed

PhD candidate

Email ahmedraed09@gmail.com

II. ^aWaleed El-Awady

PhD, Mechanical Power Engineering Department, Faculty of Engineering, Mansoura University, El-Mansoura, 35516, Egypt.

III. ^aEl-Shafei Zeidan

Associate professor, Mechanical Power Engineering Department, Faculty of Engineering, Mansoura University, El-Mansoura, 35516, Egypt.

IV. ^aMustafa Awad

Professor, Mechanical Power Engineering Department, Faculty of Engineering, Mansoura University, El-Mansoura, 35516, Egypt.

V. ^aGalal Sultan

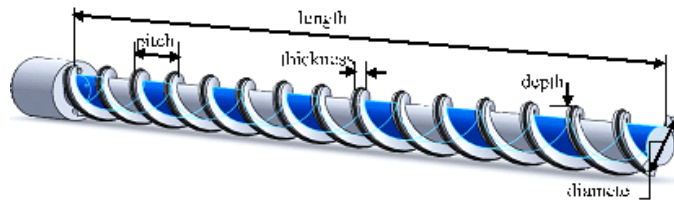
Professor, Mechanical Power Engineering Department, Faculty of Engineering, Mansoura University, El-Mansoura, 35516, Egypt.

Email gjsultan@mans.edu.eg

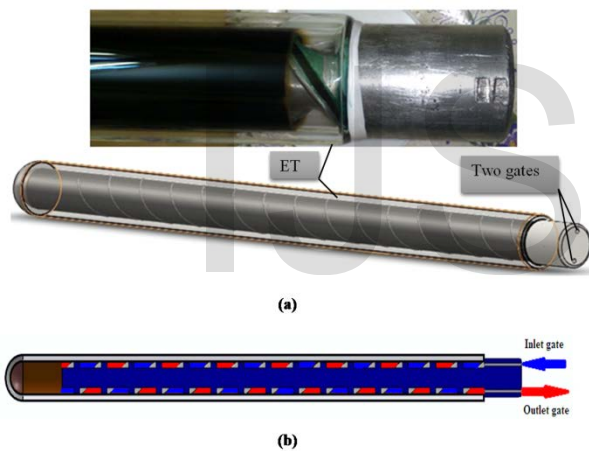
Solar energy takes more attention as a clean, free, and non-depleting source [1]. The fossil fuel power plants, which are the main source of pollution, contribute about 66% of the worldwide produced electricity [2]. Solar collectors are considered special types of heat exchangers that transform solar energy to internal energy of a transport medium. The compound parabolic collectors, ETC and PTC, keep high efficiencies even at higher collector-inlet temperatures and the commercial viability of each system depends on the initial cost of the system and the fuel price [3]. PTC can be used on a wide range of applications as seawater desalination, production of hot water and steam power generation [4]. In 1880, the first known PTC was constructed by John Ericsson [5]. In 1912, a large solar irrigation pumping plant in Meadi (Egypt) was designed and built using the PTC [5, 6]. The improvement of PTC's durability, maintenance, operation and cost reduction investigations are the main fields of recent research and the receiver performance improvements have taken the most attention [7]. Riffelmann et al. [8] presented two methods to assess the solar flux in the focal region of parabolic troughs by either detecting the concentrated sunlight by photodiodes or using the indirect camera-target methods. Other numerical simulations of the optical and thermal behavior of a PTC to assess the solar flux distribution around the receiver were also conducted [9, 10].

The geometry design parameters of the PTC strongly effect on the collector performance as aperture area, concentration ratio, rim angle, and outer diameter of the receiver [11, 12]. The collector efficiency improved by reducing the receiver diameter and increasing the mirror's active diameter [13]. The most affected parameters are the solar radiation intensity and the incidence angle which reveal opposite effect on heat collecting efficiency [14]. The solar radiation intensity has a considered effect in determining the charging time of any

storage system [15]. Also, one of the effective parameters on the collector performance is the heat transfer fluid flow rate where the thermal performance of the collector increases as the flow rate increases [14, 15]. ETCs can collect both diffuse and direct radiations and it is less affected by wind and low ambient temperature due to the enveloped vacuum between its inner and outer tubes [16]. The interlayer pressure between absorber tube and glass tube has a large effect on heat losses from the absorber tube [14]. The non-uniformity of the solar energy flux distribution on the absorber tube, in the solar energy concentrating systems, is very large [17]. This distribution can induce large thermal stress and even receiver failure [18]. Enhancing of heat transfer inside the absorber tube helps to enhance the PTC's receiver thermal performance and reduce these thermal stresses [19, 20]. Twisted-tape and helical screw-tape are common inserts that enhance heat transfer and can effectively homogenize the temperature distribution on the tube surface. Twisting and width ratios and Reynolds number are important parameters to achieve thermal performance enhancement [21-23]. The twisted-tape and helical screw-tape inserts are preferable at low Reynolds numbers and small flow rates [20, 22]. Using twisted inserts, either fitted with rod and spacer at the trailing edge [24] or fitted with straight



full twist insert [25], enhancing the collector performance compared with the plain tube one. Although the heat transfer increases and heat removal factor decreases by using the tape inserts, the pressure loss also increases [23, 26].



From the previous review, it is clear that solar collector's enhancement still needs more research work. In the present work, a novel configuration of a PTC with a helical screw tape insert is proposed. This helical screw tape insert has two-pass flow, one for inlet and the other for outlet as shown in Fig. 1. The two passes create a counter-flow heat exchanger inside the evacuated tube to increase the homogeneity of the temperature distribution along the receiving element. In addition, the heat transfer may be enhanced due to the swirl flow and due to the increasing of the residence time of the heat transfer fluid. In the present work, an experimental investigation of the PTC which has an evacuated tube receiver is performed. To assess the effect of this configuration on the parabolic trough collector performance, experiments using water as a working fluid at flow rates of 10, 12, 16, 20, and 25 L/h are performed and analyzed.

Fig. 1 Two-gate aluminum helical screw tape insert in an ET receiver: (a) photographic image; (b) front sectional view.

2 Experimental setup and experimental procedure

The PTC consists of a receiver, and parabolic reflector which are assembled together using an iron structure frame. The receiver is a commercial evacuated double glass tube with a length of 0.9 m, inner diameter of 0.043 m, and outer diameter of 0.048 m. The two layers of the glass have a thickness of 0.0016 m and a vacuum pressure between them of 5.0×10^{-3} Pa. The outer glass layer is a clear glass with a maximum transmittance, τ , of 0.95, where the other is coated with a black layer which has an absorptivity, α , of 0.93, and emissivity of

selective coating, τ , of 0.05. In order to increase the solar heat gain, a two-gate (double start) aluminum helical screw is used. This helical screw has a length of 0.74 m and a diameter of 0.0427 m, whereas the channel depth, thickness, and pitch are 0.008 m, 0.0095 m, and 0.048 m, respectively as shown in Figure 2. The HTF enters into the ET receiver, which is fitted with the two-gate aluminum helical screw tape, through inlet gate and flows swirly until the closed end of the helical screw and then returns back swirly also and exits through the outlet gate.

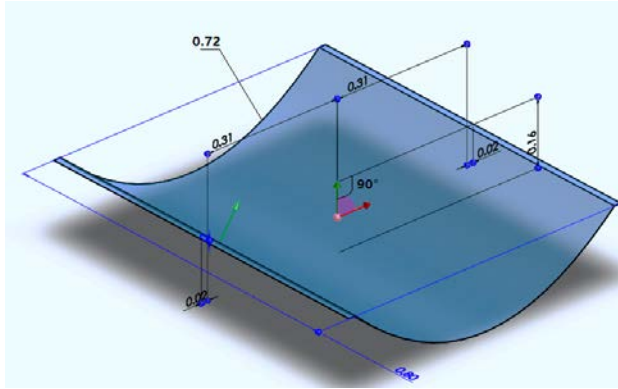


Fig. 2 Aluminum helical screw geometry.

Fig. 3 Dimensions of the reflector (all dimensions in m).

The reflector is constructed by grouping 36 pieces of glass mirror reflector which have a 0.8 m length, 0.02 m width and 0.004 m thickness. These mirror pieces are constructing a reflecting area of 0.576 m² which are supported by a parabolic iron sheet, as shown in Figure 3. The specifications of this parabolic iron sheet are given in Table 1.

Table 1
 Parabolic iron sheet specifications.

Specification	Value	Unit
Length	0.8	m
Aperture width, w	0.625	m
Focal length, f	0.1562	m
Height of concentrate, h	0.1562	m
Arc length, S_p	0.72	m
Rim angle, ψ	90	

The reflector is supported by a metallic structure, which allows the reflector to be rotated about its east-west axis to track manually the beam radiation according to the incidence angle variation during the day. The photograph of the experimental test-rig and its schematic diagram are shown in Figures 4 and 5, respectively. Three ½ inch ball valves are used to control the water flow and water pressure inside the ET, two of them are located at water inlet and outlet and the third is located after the water tank. A pressure gauge with an accuracy of $\pm 3\%$ is used to measure the water pressure. The inlet and outlet water temperatures are measured by two calibrated thermocouples type (K) of 0.5 mm diameter. These thermocouples are connected to a data logger, OM-DAQ-USP-2401 which has an accuracy of ± 1.3 °C when connected with type (K). The ambient and the water supply temperatures are measured by alcohol glass thermometers of ± 0.5 °C accuracy. The volume flow rate is measured by measuring an amount of water collected during a measured period. The total solar radiation on a horizontal surface is recorded by solar power meter TES-1333R which has an accuracy of ± 10 W/m² and range of 2000 W/m².



Fig. 4 Photograph of the experimental PTC.

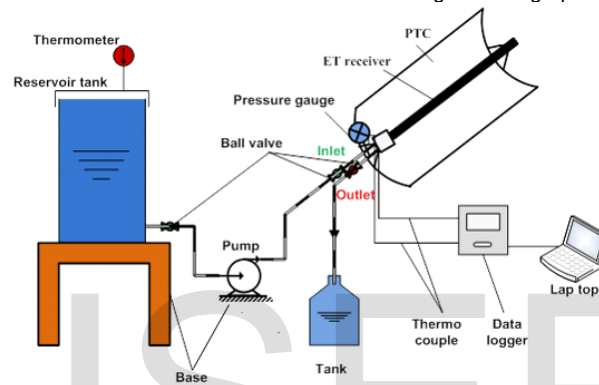


Fig. 5 Schematic diagram of the experimental test-rig.

3 Technique and Operating Conditions

The present experimental investigation is performed in Mansoura city in Egypt, which is located at 31.04 °N latitude and 31.23 °E longitude [27]. The experiments were performed in May 2016 for different five days at different flow rates (10, 12, 16, 20, and 25 L/h). At the beginning of every experiment, a pump (DELTA QB-60) with a max flow rate of 20 L/min is started up to purge the trapped air inside the system for about 5 minutes. The flow rate of water is adjusted using two ball valves at water inlet and outlet. After reaching the required flow rate, the solar reflector is rotated about its east-west axis to concentrate the solar radiation on the ET receiver.

4 Data Reduction

The control of tracking is performed manually according to the variation of calculated tracking angle as following [28]:

$$(1)$$

Where

is the angle between the plane of the surface and the horizontal, the zenith angle, and the solar azimuth angle.

The real time of the data logger and the solar radiation recorder are adjusted to prevent mismatching between the different measured data. The inlet and outlet water temperatures are recorded by the data logger for 5 seconds step, and the solar radiation is recorded by solar power meter TES-1333R on the horizontal surface for 28 seconds step.

The instantaneous efficiency of the PTC is calculated using the following equation [28]:

$$(2)$$

Where

is the beam radiation, R_b the geometric factor and A_c the aperture area of the collector.

By integrating Eq. (2), the hourly efficiency and the average daily efficiency of the PTC can be obtained.

$$(3)$$

$$(4)$$

The heat removal factor, which can be defined as the ratio of the actual useful energy gain to the useful energy gain if the whole water temperature along the ET is at the water inlet temperature can be calculated as following [28]:

$$(5)$$

Where

is the area of the absorber, U_L overall heat loss coefficient, T_a ambient temperature, and S the absorbed solar radiation per unit surface area.

Thus, the PTC efficiency can be rewritten as following:

$$(6)$$

When the least squares fit is applied to the experimental data, a linear relation between η and $(T_w - T_a)/T_w$ is obtained. Using this linear fit and equation (6) for PTC efficiency, the heat removal factor can be obtained.

5 Results and discussion

Figure 6 shows the incident solar radiation for the five experiment days to depict the degree of solar radiation variation at all experiment days.

It can be observed that the maximum variation between the measured mean hourly incident solar radiations during the experiment days is about 14%.

Fig. 6 Mean hourly incident solar radiation during experiment days.

Figures 7 and 8 depict the recorded ambient and inlet temperatures during the experiment days, respectively. For the ambient temperature, the maximum recorded temperature difference is about 7 °C between all experiments except the 20 L/h which records a maximum temperature difference of 17 °C. While for the inlet water temperature, the maximum inlet temperature difference between all experiments is about 6 °C.

Fig. 7 Mean hourly ambient temperature variation during the different experiment days.

Fig. 8 Mean hourly inlet water temperature variation for different flow rates.

Figure 9 shows the outlet and inlet water temperature difference for all experiments. The maximum water temperature difference is recorded at the minimum flow rate 10 L/h which has a value of 24 °C, where the minimum peak occurs at the maximum flow rate 25 L/h which has the value 10 °C.

Fig. 9 Water temperature difference variation for different flow rates.

Figure 10 indicates the variation of the hourly collector efficiency at flow rates (10-25) L/h. It can be observed that the hourly collector efficiency takes the same trend of the total incident solar radiation for all experiment days except the experiment of 10 L/h flow rate. For this flow rate the hourly collector efficiency takes the same trend as all other days from the beginning of the experiment till 15:30 h. After 15:30 h the solar radiation is sharply decreased due to a cloudy weather where the hourly collector efficiency increases and

reaches higher values. This thermal behavior may be explained as when the solar radiation decreases sharply the solar heat gain (\dot{Q}_s) decreases and at the same time the useful energy (\dot{Q}_u) still increasing due to the heat absorbed from the stored heat in the aluminum helical screw core.

Fig. 10 Hourly PTC efficiency for all flow rates.

This behavior reflects that the helical screw core may be used as thermal storage, which enhances the solar collector performance during the cloudy periods and it can compensate the effect of the large instantaneous variation of the incident solar radiation. It is found that the maximum hourly efficiency is 84.5% at 20 L/h experiment, and the minimum hourly efficiency is 27.1% at 12 L/h experiment.

The daily cumulative incident energy on the aperture of the PTC and the PTC energy gain during the test hours at flow rates 10 and 20 L/h are shown in Figures 11 and 12, respectively. It can be seen from these figures that the PTC energy gain increases with increasing the incident energy on the aperture of the PTC, except the period from 15:30 h to 17:00 h at flow rate 10 L/h in Figure 11. At this period, it can be noticed that the rate of increase of the incident energy is less than the rate of increase of the PTC energy gain. This is because of decreasing in the total incident solar radiation, due to cloudy weather and the stored heat in the aluminum helical screw, in addition to the low flow rate of water, which explains the increase of hourly collector efficiency to higher values in that period.

Fig. 11 Hourly variation of cumulative incident solar energy falls on the aperture of the PTC and the PTC energy gain at 10 L/h experiment day, 17/5/2016.

Fig. 12 Hourly variation of cumulative incident solar energy falls on the aperture of the PTC and the PTC energy gain at 20 L/h experiment day, 14/5/2016.

Daily efficiency determines the performance of the PTC; the daily efficiency is defined as the ratio of the useful energy delivered to the working fluid per energy incident on the aperture of the trough, during the day. This parameter is important to evaluate the system output, in addition to the performance parameters for PTC (heat removal factor and overall heat loss coefficient). Table 2 shows the average daily efficiency of all experiment days versus the water flow rate, where the other parameters as the total incident solar radiation, ambient temperature, inlet water temperature, in the present study, have a relatively small variation.

Table 2
 The PTC average daily efficiency of all experiment days.

Flow rate, (L/h)	10	12	16	20	25
(%)	60.43	61.77	59.48	69.06	63.83

Table 3 indicates the performance parameters for the PTC at flow rates 10, 12, 16, 20, and 25 L/h and depicts that the minimum heat removal factor and minimum overall heat loss coefficient occur at flow rate 20 L/h which agree with the results of hourly and daily efficiency curves.

Table 3
 The performance parameters for the PTC.

Performance parameters	Flow rate (L/h)				
	10	12	16	20	25
	0.90512	1.33237	1.07837	0.84275	0.893
(W/m ² °C)	12.4678	29.8084	43.7714	9.637	25.7368

6 Error analysis

The uncertainty analysis for the calculated parameters such as water mass flow rate, projected area, beam radiation, temperature differences, and daily efficiency based on the the measured parameters accuracies as temperature, lengths, and solar radiation is performed. The resulted uncertainties for the calculated parameters are shown in Table 4.

Table 4
 The uncertainty analysis for the calculated parameters.

Parameters					
Uncertainty (%)					

7 Conclusions

A parabolic trough solar collector (PTC) with two-gate helical screw-tape inserts receiver is designed and manufactured. The performance of the PTC is carried out at different flow rates of 10, 12, 16, 20, and 25 L/h. From the experimental results, it can be concluded that:

- The maximum water temperature difference is recorded at the minimum flow rate 10 L/h which has a value of 24 °C, where the maximum hourly efficiency is 84.5% at 20 L/h experiment day.
- The helical screw core may be used as a thermal storage, which enhance the solar collector performance during the cloudy periods and it can compensate the effect of the large instantaneous variation of the incident solar radiation.
- The maximum daily efficiency is 69.06% at 20 L/h experiment day while the minimum daily efficiency is 59.48% at 16 L/h experiment day.
- The minimum heat removal factor and minimum overall heat loss coefficient occur at flow rate 20 L/h which agree with the results of hourly and daily efficiency curves.

Nomenclature

	Area of aperture of the PTC	m ²
	Area of the absorber	m ²
	Water heat capacity	J/kg °C
	Focal length	m
	Heat removal factor	----
	Height of concentrate	m
	Beam radiation	W/m ²
	Water flow rate	kg/s
	Geometric factor	----
	Solar radiation absorbed by the solar collector per unit surface area	W/m ²
	Arc length	m
	Ambient temperature	°C
	Water inlet temperature	°C
	Water outlet temperature	°C
U_L	Overall heat loss coefficient	W/m ² C
	Aperture width	m
Abbreviations		
ET	Evacuated Tube	
ETC	Evacuated Tube Collector	
HTF	Heat Transfer Fluid	
PTC	Parabolic Trough Collector	
Greek symbols		
	Evacuated tube absorptance	----
	Angle between the plane of the surface and the horizontal	°
	Solar azimuth angle	°
	Hourly efficiency	%

	Daily efficiency	%
	Instantaneous efficiency	%
	Zenith angle	°
	Transmittance	-----
	Daily average transmittance- absorptance	-----
ψ	Rim angle	°
Subscripts		
	Aperture, ambient	
	Beam	
	Daily	
	Evacuated tube	
	Instantaneous	
T	Time	
w_i	Water inlet	
w_o	Water outlet	

References

- E. Hu, Y. Yang, A. Nishimura, F. Yilmaz, and A. Kouzani, "Solar thermal aided power generation," *Appl. Energy*, vol. 87, pp. 2881–2885, 2010.
- M. S. Jamel, A. Abd Rahman, and A. H. Shamsuddin, "Advances in the integration of solar thermal energy with conventional and nonconventional power plants," *Renew. Sustain. Energy Rev.*, vol. 20, pp. 71–81, 2013.
- S. Kalogirou, "The potential of solar industrial process heat applications," *Appl. Energy*, vol. 76, no. 4, pp. 337–361, 2003.
- S. A. Kalogirou, "A detailed thermal model of a parabolic trough collector receiver," *Energy*, vol. 48, no. 1, pp. 298–306, 2012.
- J. T. Pytlinski, "solar energy installations for pumping irrigation water," *Sol. Energy*, vol. 21, pp. 255–262, 1978.
- J. F. Kreider and F. Kreith, *Solar energy handbook*. McGraw-Hill Book Company, New York, NY, 1981.
- A. Mwesigye, T. Bello-Ochende, and J. P. Meyer, "Heat transfer and thermodynamic performance of a parabolic trough receiver with centrally placed perforated plate inserts," *Appl. Energy*, vol. 136, pp. 989–1003, 2014.
- K. J. Riffelmann, A. Neumann, and S. Ulmer, "Performance enhancement of parabolic trough collectors by solar flux measurement in the focal region," *Sol. Energy*, vol. 80, no. 10, pp. 1303–1313, 2006.
- A. A. Hachicha, I. Rodríguez, R. Capdevila, and A. Oliva, "Heat transfer analysis and numerical simulation of a parabolic trough solar collector," *Appl. Energy*, vol. 111, pp. 581–592, 2013.
- G. Coccia, G. Latini, and M. Sotte, "Mathematical modeling of a prototype of parabolic trough solar collector," *J. Renew. Sustain. Energy*, vol. 4, no. 2, p. 23110, 2012.
- S. P. and Sukhatme and J. K. Nayak, *Solar Energy: Principles of Thermal Collection and Storage*. Tata McGraw-Hill Publishing Company, 2008.
- G. M. Mufti, D. Naeem, and A. Waqas, "Optimization of physical dimensions for efficient Parabolic Trough Collectors using mathematical and computational models," *International Conference on Modeling and Simulation*, Nov. 25–27, Islamabad, Pakistan, 2013.
- G. C. Bakos, I. Ioannidis, N. F. Tsagas, and I. Seftelis, "Design, optimisation and conversion-efficiency determination of a line-focus parabolic-trough solar-collector (PTC)," *Appl. Energy*, vol. 68, no. 1, pp. 43–50, 2001.
- Y.-L. He, D.-H. Mei, W.-Q. Tao, W.-W. Yang, and H.-L. Liu, "Simulation of the parabolic trough solar energy generation system with Organic Rankine Cycle," *Appl. Energy*, vol. 97, pp. 630–641, 2012.
- G. Kumaresan, R. Sridhar, and R. Velraj, "Performance studies of a solar parabolic trough collector with a thermal energy storage system," *Energy*, vol. 47, no. 1, pp. 395–402, 2012.
- M. A. Sabiha, R. Saidur, S. Mekhilef, and O. Mahian, "Progress and latest developments of evacuated tube solar collectors," *Renew. Sustain. Energy Rev.*, vol. 51, pp. 1038–1054, 2015.
- Z. D. Cheng, Y. L. He, and F. Q. Cui, "Numerical study of heat transfer enhancement by unilateral longitudinal vortex generators inside parabolic trough solar receivers," *Int. J. Heat Mass Transf.*, vol. 55, no. 21–22, pp. 5631–5641, 2012.
- W. Fuqiang, T. Jianyu, M. Lanxin, and W. Chengchao, "Effects of glass cover on heat flux distribution for tube receiver with parabolic trough collector system," *Energy Convers. Manag.*, vol. 90, pp. 47–52, Jan. 2015.
- M. A. Irfan and W. Chapman, "Thermal stresses in radiant tubes due to axial, circumferential and radial temperature distributions," *Appl. Therm. Eng.*, vol. 29, no. 10, pp. 1913–1920, 2009.
- X. Song, G. Dong, F. Gao, X. Diao, L. Zheng, and F. Zhou, "A numerical study of parabolic trough receiver with nonuniform heat flux and helical screw-tape inserts," *Energy*, vol. 77, pp. 771–782, 2014.

- A. Mwesigye, T. Bello-Ochende, and J. P. Meyer, "Heat transfer and entropy generation in a parabolic trough receiver with wall-detached twisted tape inserts," *Int. J. Therm. Sci.*, vol. 99, pp. 238–257, 2016.
- O. A. Jaramillo, M. Borunda, K. M. Velazquez-Lucho, and M. Robles, "Parabolic trough solar collector for low enthalpy processes: An analysis of the efficiency enhancement by using twisted tape inserts," *Renew. Energy*, vol. 93, pp. 125–141, 2016.
- S. Bhattacharyya, H. Chattopadhyay, S. Bandyopadhyay, and S. Roy, "Experimental Investigation on Heat Transfer Enhancement by Swirl Generators in a Solar Air Heater Duct," *Int. J. HEAT Technol.*, vol. 34, no. 2, pp. 191–196, 2016.
- S. Jaisankar, T. K. Radhakrishnan, and K. N. Sheeba, "Experimental studies on heat transfer and friction factor characteristics of thermosiphon solar water heater system fitted with spacer at the trailing edge of twisted tapes," *Appl. Therm. Eng.*, vol. 29, no. 5–6, pp. 1224–1231, 2009.
- S. R. Krishna, G. Pathipaka, and P. Sivashanmugam, "Heat transfer and pressure drop studies in a circular tube fitted with straight full twist," *Exp. Therm. Fluid Sci.*, vol. 33, no. 3, pp. 431–438, 2009.
- S. Eiamsa-ard and P. Promvong, "Enhancement of heat transfer in a tube with regularly-spaced helical tape swirl generators," *Sol. Energy*, vol. 78, pp. 483–494, 2005.
- Egypt Latitude and Longitude Map. http://www.mapsofworld.com/lat_long/egyptlat-long.html. Last day accessed 6 June. 2018.
- J. a. Duffie and W. a. Beckman, *Solar Engineering of Thermal Processes*, 4th Edition, John Wiley & Sons, 2013.

IJSER